

# SIBILA: High-performance computing and interpretable machine learning join efforts toward personalised medicine in a novel decision-making tool

Antonio Jesús Banegas-Luna<sup>a,\*</sup>, Horacio Pérez-Sánchez<sup>a</sup>

<sup>a</sup> Structural Bioinformatics and High-Performance Computing Research Group (BIO-HPC), Universidad Católica de Murcia (UCAM), Murcia 30107, Spain

## Keywords

deep learning, high-performance computing, explainable artificial intelligence, personalised medicine, consensus, decision-making

## Abstract

### Background and Objectives

Personalised medicine remains a major challenge for scientists. The rapid growth of Machine learning and Deep learning has made it a feasible alternative for predicting the most appropriate therapy for individual patients. However, the lack of interpretation of their results and high computational requirements make many reluctant to use these methods.

### Methods

Several Machine learning and Deep learning models have been implemented into a single software tool, SIBILA. Once the models are trained, SIBILA applies a range of interpretability methods to identify the input features that each model considered the most important to predict. In addition, all the features obtained are put in common to estimate the global attribution of each variable to the predictions. To facilitate its use by non-experts, SIBILA is also available to all users free of charge as a web server at <https://bio-hpc.ucam.edu/sibila/>.

### Results

SIBILA has been applied to three case studies to show its accuracy and efficiency in classification and regression problems. The first two cases proved that SIBILA can make accurate predictions even on uncleaned datasets. The last case demonstrates that SIBILA can be applied to medical contexts with real data.

### Conclusion

With the aim of becoming a powerful decision-making tool for clinicians, SIBILA has been developed. SIBILA is a novel software tool that leverages interpretable machine learning to

make accurate predictions and explain how models made those decisions. SIBILA can be run on high-performance computing platforms, drastically reducing computing times.

## 1. Introduction

The rapid development of technologies has helped artificial intelligence (AI) become a well-known and reliable tool for researchers in academia and industry. Its ability to analyse vast amounts of data has become a powerful tool in science and businesses. Looking for repetitive patterns among such datasets is a complex but necessary task that needs to be done to extract knowledge from past events. Once the rules managing raw data have been identified, AI models can use them to make predictions about new unexplored samples.

Machine learning (ML) and deep learning (DL) are the two types into which AI models are often classified [1], depending on the complexity of the algorithm used. Both types of models are flexible enough to analyse a range of datasets, including tabular data, time series and images. This adaptability to different contexts has propelled their application in traditional and fundamental areas of science, such as biology [2,3], chemistry [4,5] and medicine [6]. But not only classical scientific areas can profit from ML and DL, but also new and related multidisciplinary fields. This is the case for genomics [7,8], bioinformatics [9] and drug discovery [10-12], to name a few.

Of all the scientific areas mentioned, medicine is probably the one with the highest visibility in society. Advances related to medicine are frequently considered highly relevant; therefore, any help is always welcome. Consequently, how ML and DL help learn how diseases could be cured or treated is a timely topic. As a result, more than a few examples of both methods applied to medicine can be found in the literature. Pérez-Gandía et al. [13] developed a decision support system that helps patients with type 1 diabetes mellitus to monitor their glucose levels daily. This way, abnormal situations can be anticipated, and measures can be taken earlier than a traditional follow-up.

Evaluating and predicting therapy outcomes may be of great help for doctors in decision making. An extensive revision of works about outcome prediction in patients with depression was made by Lee et al. [14]. Even more dramatic than mood disorders is the incidence of cancer in the population. Early detection is often believed to be the most effective treatment. Hence it is one of the significant targets of DL when applied to cancer therapy. In the case of colorectal cancer (CRC), the effectiveness of colonoscopy is measured by its adenoma detection rate, which can be increased by using convolutional neural networks (CNN) for image processing [15]. Furthermore, ML algorithms can predict the presence of lymph node metastasis, which represent a risk factor for patients who need surgery, therefore reducing the number of unnecessary surgeries [16]. Although many other works applied ML and DL algorithms to medical contexts, being able to adapt a standard therapy to an individual patient, the so-called personalised therapies, remains a challenge [17-20].

Although DL models are a powerful tool for decision making in medicine and the number of clinical studies in the field of ML has grown a lot in the last years [21], they still lack the level of interpretation required to be understood by physicians. Thus, an extra layer should be added on top of the architecture to make the raw predictions provided by the models easier to

understand by the general public. Additionally, this extra layer increases the computational resources, programming complexity and user interactivity difficulties required to train the model and make predictions. The models would have to be run on high-performance computing (HPC) platforms, and even then, the whole process might take several hours or days [22].

In this paper, and to solve previously described problems, we describe SIBILA, a command-line code that implements a novel ML and DL engine that can be run locally or on a supercomputing platform, resulting in very competitively response times and ease of use. Moreover, it applies a diversity of interpretability methods to provide the final user with a deep insight into the decisions that led the model to make a prediction. In addition, SIBILA functionalities are also available through a freely accessible web server at <https://bio-hpc.ucam.edu/sibila/>. Three case studies will be presented in this paper to discuss and prove the effectiveness of the models.

## 2. Materials and Methods

This section describes the main features of SIBILA, including the ML/DL models and interpretability methods available, how the consensus works and its implementation in HPC. SIBILA has been programmed in python3, and it relies on a set of widely used libraries to implement both the models and interpretability methods.

### 2.1. Machine learning and deep learning models

SIBILA implements a collection of ML and DL models in a flexible way that could easily be extended in the future. Table 1 summarises the available models, algorithms, libraries and whether they support regression and classification.

**Table 1.** List of models and algorithms implemented by SIBILA.

MODEL	NAME	LIBRARY	CLASSIFICATION	REGRESSION
DT	Decision Tree	scikit-learn	Yes	Yes
RF	Random Forest	scikit-learn	Yes	Yes
SVM	Support Vector Machine	scikit-learn	Yes	Yes
XGBOOST	eXtreme Gradient Boosting	xgboost	Yes	Yes
KNN	K-Nearest Neighbours	scikit-learn	Yes	Yes
ANN	Artificial Neural Network	TensorFlow 2	Yes	Yes
RIPPER	Repeated Incremental Pruning to Produce Error Reduction	Wittgenstein	Yes	No
RLF	RuleFit	refit	Yes	No

All models, except ANN, perform an automatic grid search which means that SIBILA tries several model configurations and chooses the best one. The case of ANN is different because of the difficulties of creating different topologies. Therefore, an “*external*” grid search method is implemented, which generates a JSON file for each model.

## 2.2. Evaluation metrics

To assess the accuracy of the models, some metrics are calculated based on the test data. Since different metrics measure classification and regression problems, a good set has been implemented in SIBILA. Table 2 lists all available metrics.

**Table 2.** Evaluation metrics for classification and regression problems.

CLASSIFICATION	REGRESSION
Confusion matrix Accuracy Precision F1 score Recall Specificity Area Under the Curve (AUC)	Pearson coefficient Coefficient of determination ( $R^2$ ) Mean average precision Mean absolute error (MAE) Mean squared error (MSE)

## 2.3. Interpretability methods

As well as performance metrics, many interpretability algorithms are employed to detect the most relevant input features, their relevance and, in some cases, their positive or negative contribution. Table 3 summarises these algorithms. It is not the aim of this manuscript to go into the algorithms; therefore, only those details that are relevant for understanding the output of SIBILA will be given. Additionally, all information regarding the attributions calculated by the algorithms is bulked into CSV files so that users can see the raw data provided by SIBILA. They can then use it for further analysis.

**Table 3.** Interpretability methods are available.

METHOD	LIBRARY	REF
Permutation importance	scikit-learn	[23, 24]
Local Interpretable Model-Agnostic Explanations (LIME)	lime	[24, 25]
Shapley values	shap	[24, 26]
Integrated gradients	alibi	[27]
Diverse Counterfactual Explanations (DiCE)	dice-ml	[24, 28]
Partial Dependence Plot (PDP) + Individual Conditional Expectation (ICE)	scikit-learn	[24, 29]
Accumulated Local Effects (ALE)	alibi	[24, 30]

While PDP and ALE create individual graphs for each input variable, the rest of the methods make one graph displaying the attribution of all inputs. Additionally, since LIME, Shapley values, integrated gradients, and DiCE plot attributions by individual samples, it was decided

to add a global graph to display the average attribution of the variables across all samples. This way users have an overview of the global attribution of each input.

## 2.4. Execution on HPC platforms

As mentioned above, SIBILA offers the possibility to be run either locally or in a parallel environment. To facilitate its execution and increase its portability, a Singularity [31] image containing all the dependencies required by the engine was created. This way, it can be run on any computer that supports Singularity.

Singularity was chosen as the container because of the current trend of using Singularity instead of Docker in most HPC infrastructures [32] and because of the availability on most of the supercomputing platforms we have access to. Besides, SIBILA supports the *queue* parameter (-q), which allows the execution of each interpretability algorithm on a separate node of the HPC platform. This way of working dramatically reduces the time needed to obtain the results.

## 2.5. Consensus

SIBILA can run several models on the same dataset and, for each model, a collection of interpretability models is calculated. Having generated such a large amount of data, it can be challenging to identify the most relevant input features to make a decision. In addition, different models and algorithms may return different results, leading to inconsistencies.

To reduce uncertainty in interpreting results, a consensus stage was implemented. The three types of consensus provided by SIBILA are introduced. As proposed in a recent study [33], a synthetic dataset for binary classification was created to simulate a real input. The dataset, consisting of 17 input variables with values in the range [0,1] and 1948 samples, was built with some hidden rules to determine the output class (Eq. 1). The aim of our tests was to identify such rules with the consensus functionality. Once interpretability was calculated, the consensus was executed.

$$class = (if\ 0.7 \leq F3 \leq 0.9) \text{ AND } (0.2 \leq F6 \leq 0.35) \text{ then } 1 \text{ else } 0$$

**Equation 1.** Rules implemented in the test dataset.

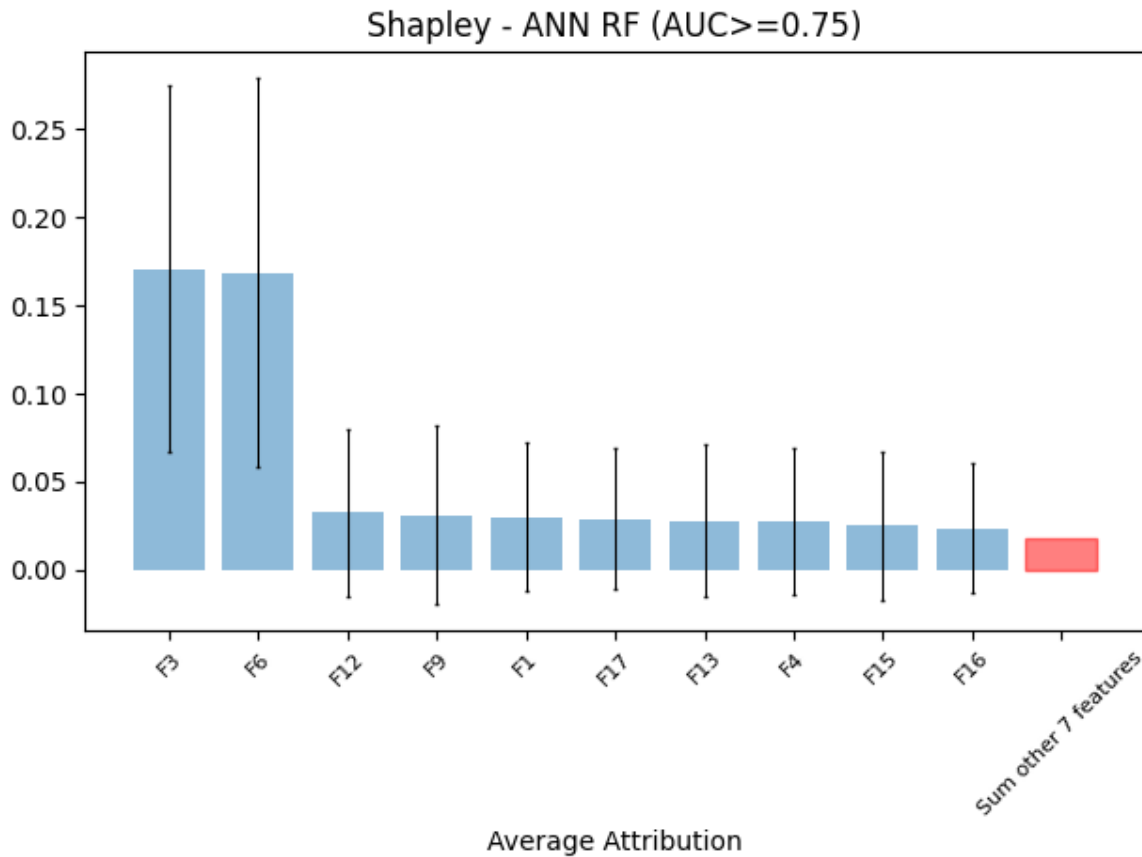


**Figure 1.** Consensus is calculated by the attribution given by one single interpretability method on many models.

Firstly, for each interpretability method, the attributions of the inputs for each model are averaged (Fig. 1). Since models with a low AUC may not be reliable, a cut-off is introduced to disregard them and avoid wrong interpretations. The default cut-off is 0.75, but the users can modify it. According to Shapley values, as shown in Figure 1, F6 and F3 are the most relevant features because they have been given the highest attributions.

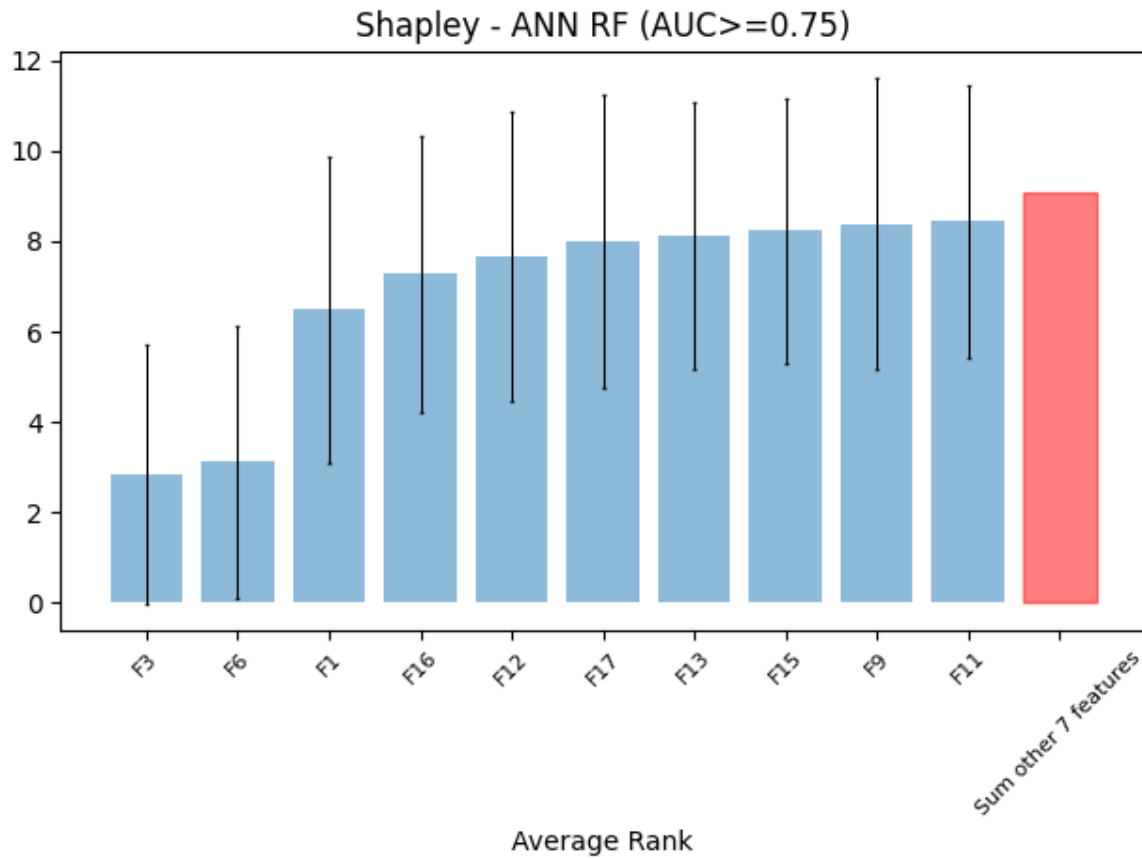


**Figure 2.** Consensus is calculated by the ranking established by one single interpretability method on many models.

Although the attributions may be the best metric for assessing the importance of the variables, the different methods applied may not be aligned, resulting in unequal attribution values. Based on this assumption, the second type of consensus averages the ranking of the input variables (Fig. 2). Again, Figure 2 shows that F6 and F3 are clearly the best ranked features and, consequently, the most important ones.

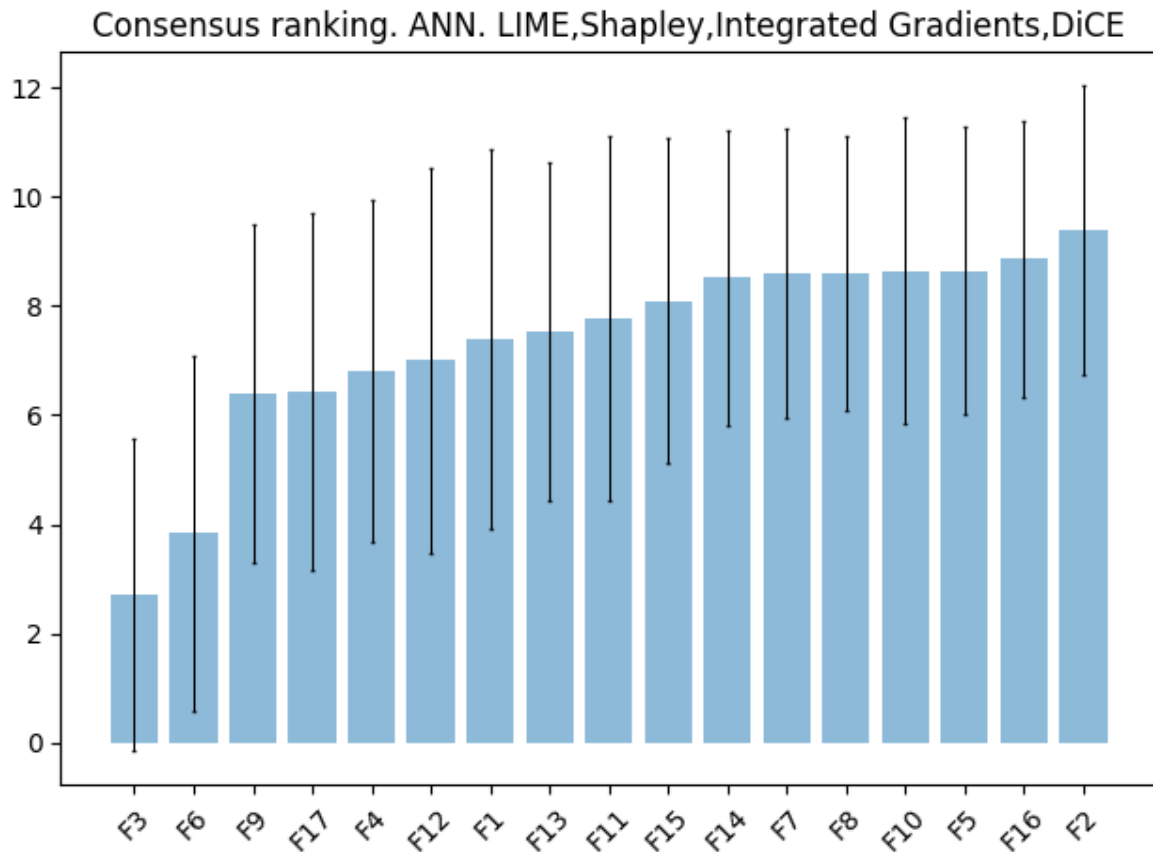


**Figure 3.** Consensus is calculated by the ranking given to one single model by many interpretability methods.

Finally, instead of grouping by interpretability method, all the explanations obtained for a given model are merged (Fig. 3). Note that this consensus is based on the ranking of the features because each interpretability algorithm ranks attributions on a different scale. According to this calculation, F6 and F3 remain the most important features when using the ANN model.

## 2.6. Code modularisation

The code of SIBILA has been conceived to be modular and flexible to be extended in the future. Based on this idea, different modules were implemented (Fig. 4). The blue boxes represent the modules the code is structured in. They are all surrounded by a continuous red line meaning that they are integrated into the core of SIBILA. In addition, some scripts are provided for pre- and post-processing tasks, such as the encoding of a dataset with the one-hot encoding technique, the creation of synthetic datasets following a given set of rules and the calculation of three types of consensus.

When using the *queue* parameter, the interpretability algorithms are executed in parallel, as shown in Figure 5.

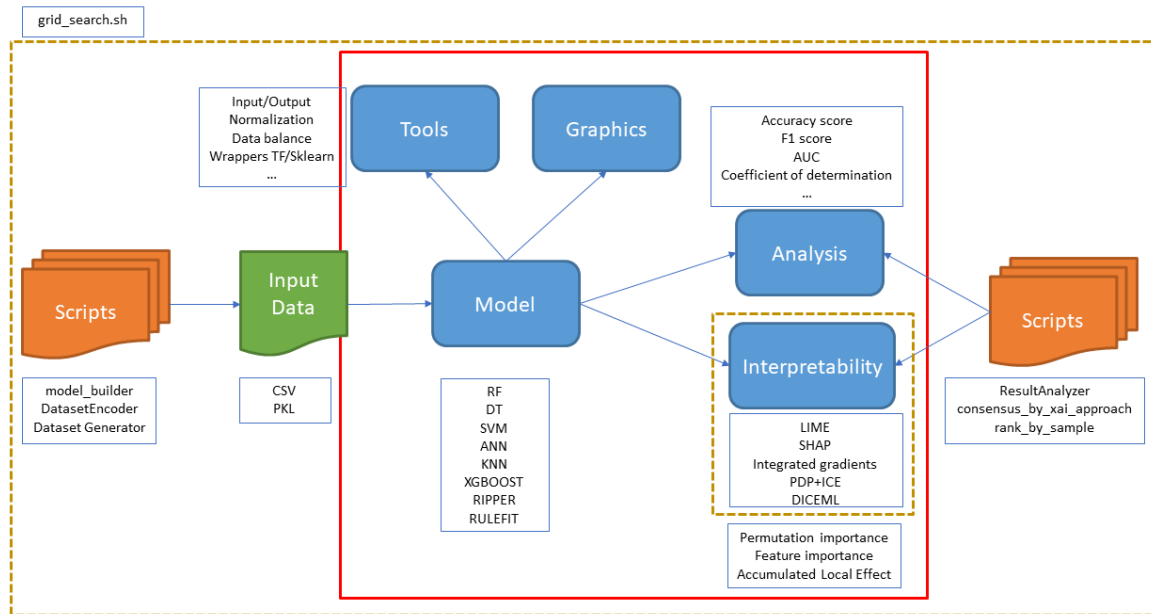


Figure 4. Schematic representation of the SIBILA modules.

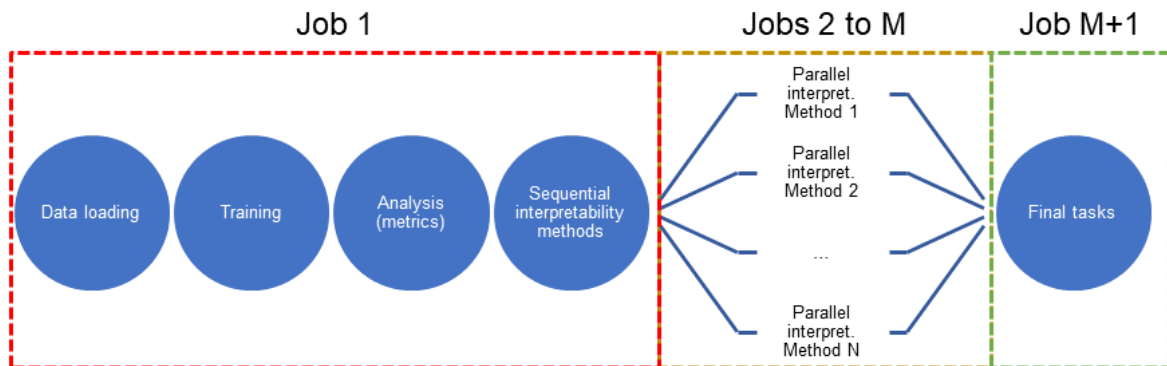


Figure 5. Parallelisation of interpretability algorithms in SIBILA.

### 3. Results

This section introduces SIBILA through three case studies. The aim of the first two samples is to show the ability of SIBILA to make predictions in both classification and regression problems. Finally, we demonstrate that SIBILA is useful in the medical field. It is used to predict the chances of suffering from a heart attack.

#### 3.1. Bike rental prediction

The first case study is based on Molnar [24]. We use SIBILA to estimate the number of bike rentals in the future and identify what features lead to such predictions. We tested all the models supporting the regression and chose the coefficient of determination ( $R^2$ ) as the metric to assess the accuracy of the models. We observed that ANN ( $R^2=1$ ), XGBOOST( $R^2=1$ ) and RF ( $R^2=0.999$ ) outperformed the other models; therefore, the consensus was calculated for them to identify the most relevant features.

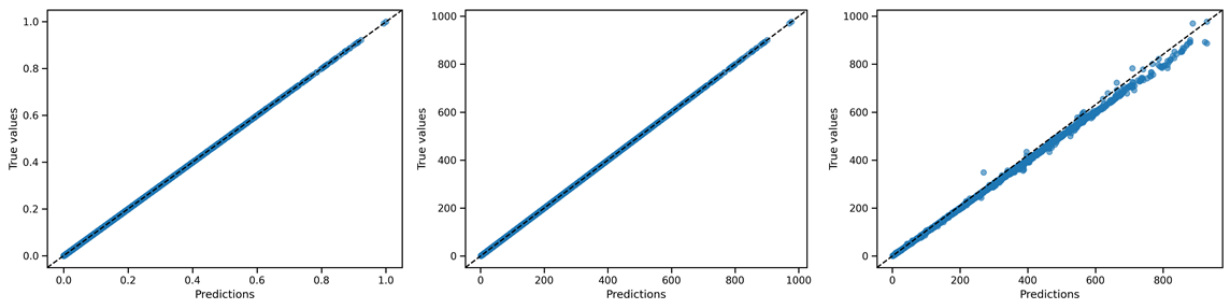


**Figure 6.** Correlation between actual and predicted values for ANN (left), XGBOOST (middle) and RF (right) models.

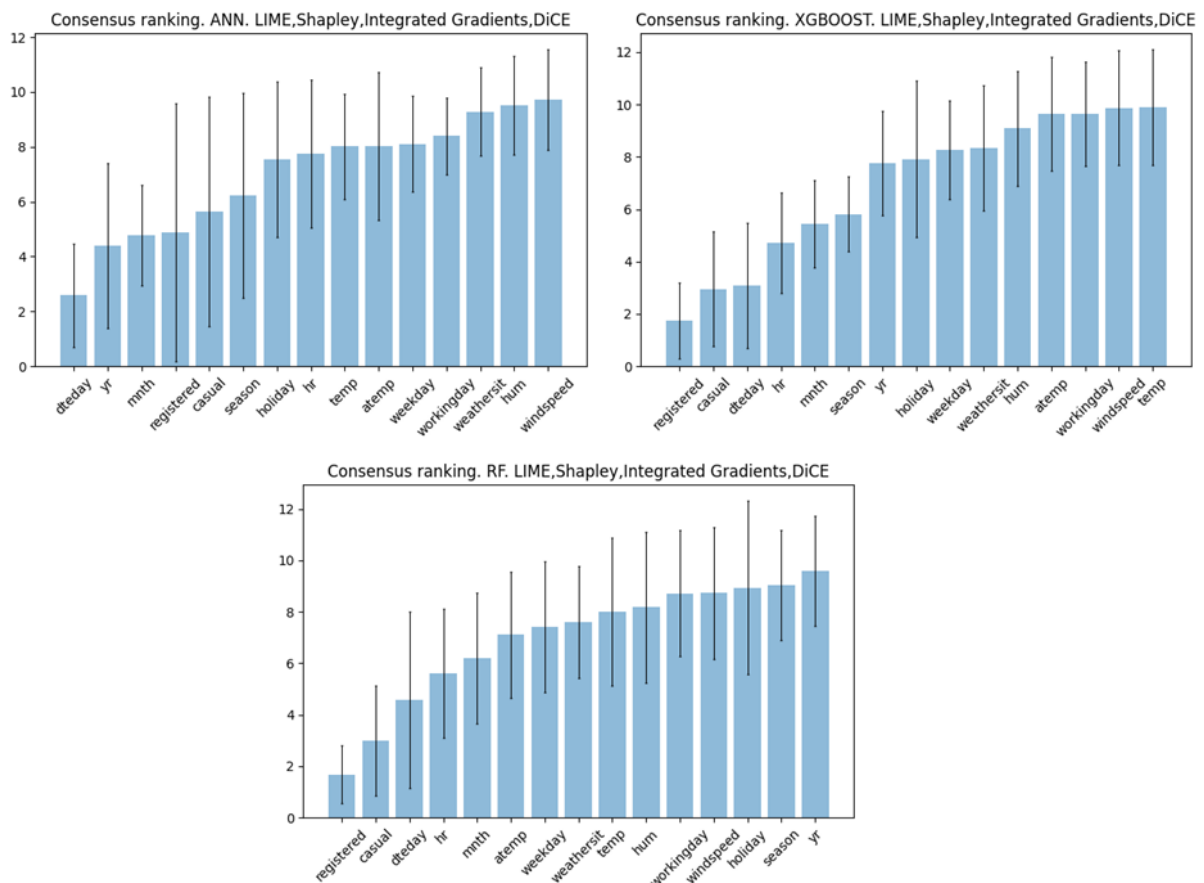


**Figure 7.** List of the most relevant features for ANN, XGBOOST and RF models.

According to ANN, the date is the most important feature, followed by the closely related year and month. Subsequently, the number of registered and casual users seems to be relevant. XGBOOST pays attention to the number of registered and casual users and the reservation date. RF returns the same explanation as XGBOOST. In short, it can be said that the number of rentals is closely linked to the number of reservations and the date, which indicates that depending on the season, people may feel like making a reservation or not.

Regarding computational cost, RF and XGBOOST took almost 1 minute to be trained, while ANN only needed 11 seconds. The low number of epochs and validation splits required to find the optimal solution made the network very efficient. Once the models were trained, our tool computed interpretability, taking 58 minutes to explain the results for RF and XGBOOST and

90 minutes to build explanations for ANN. In this case, the interpretable nature of RF and XGBOOST accelerated this stage.

### 3.2. Robustness of predictions in noisy datasets

To prove how SIBILA can distinguish between valuable and noisy data, a synthetic dataset was created for a binary classification problem. The dataset contains 2000 samples and 100 input features with values between 0 and 1. The output class is calculated according to Eq. 2.

$$class = \text{if } ((0.1 \leq F4 \leq 0.5) \text{ AND } (F10 \geq 0.6) \text{ AND } (F20 \leq 0.8) \text{ AND } (F31 \leq 0.25) \text{ AND } (0.4 \leq F57 \leq 0.7) \text{ AND } (F85 \geq 0.4)) \text{ then } 1 \text{ else } 0$$

**Equation 2.** Rules implemented in the test dataset.

Working with this dataset, we expect SIBILA to identify F4, F10, F20, F31, F57 and F85 as the most indicative features. Any subset of these variables would also be considered a good approximation because there could be unknown hidden dependencies in the data.

First, all models were trained, with ANN, RF, RLF, RP, SVM and XGBOOST obtaining the perfect classification (AUC=1). In addition, KNN also returned a high classification rate (AUC=0.976). Secondly, we ran the consensus scripts, which produced the expected result (Figure 8).

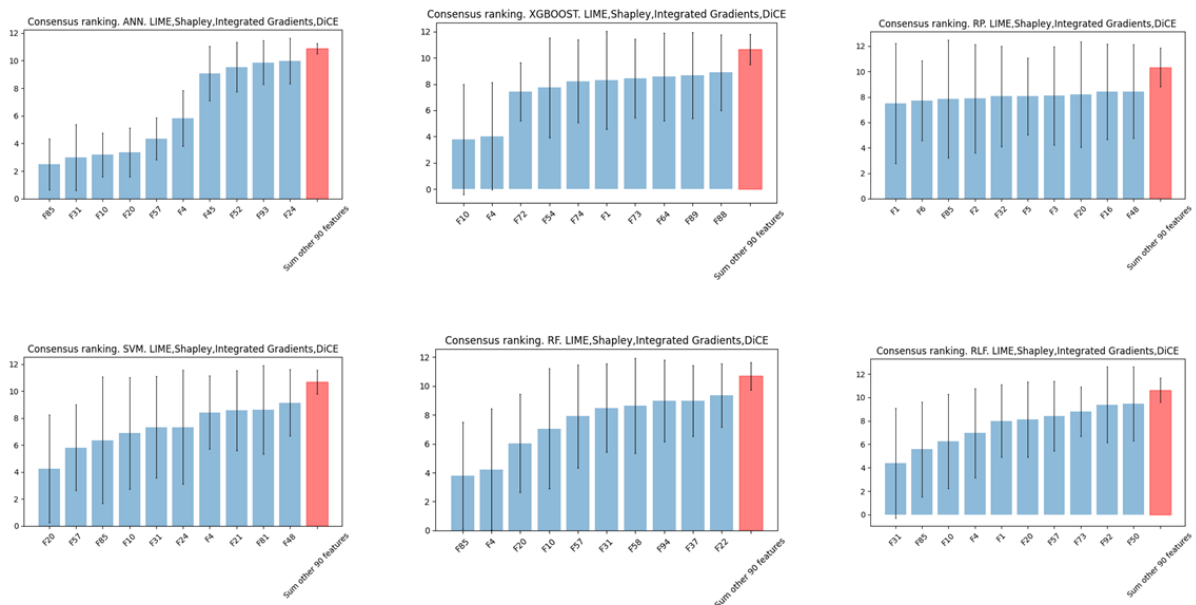


**Figure 8.** The consensus was obtained from the six perfect classifiers (ANN, XGBOOST, RP, SVM, RF, RLF).

Results prove that at least four of the six selected models have identified the six features ruling the dataset. Moreover, ANN and RF identified all the variables as the top ranked ones, while RLF and SVM found them among the top seven.

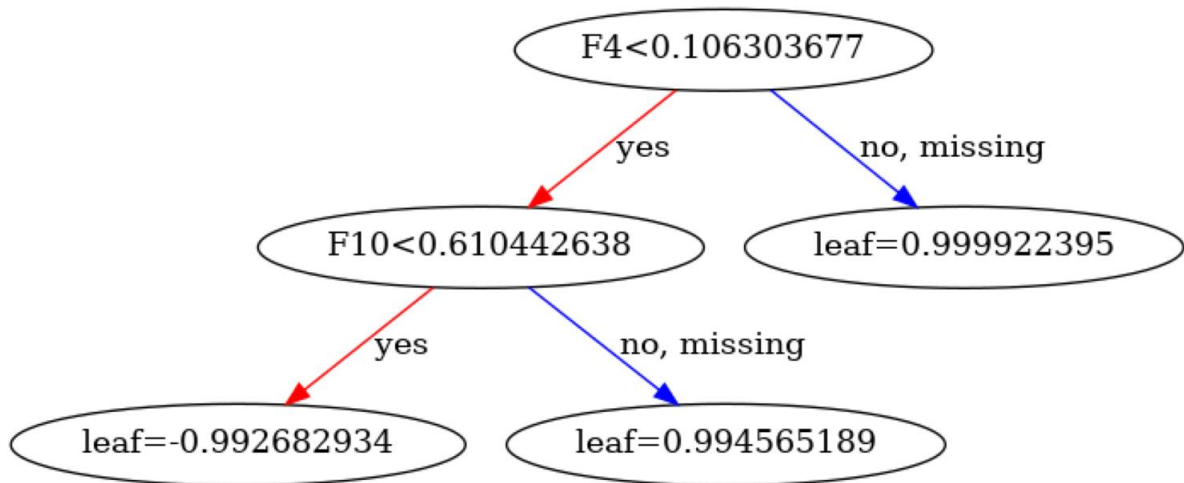


**Figure 9.** The boosting machine model clearly segregated the samples based on F4 and F10. Edge values (F4 → 0.1 and F10 → 0.6) match Eq. 2.

Finally, we examine in detail those models based on rules, with the intention of discovering edge values. The boosting machine model clearly separates the samples by a cut-off value of F4 and F10 (Fig. 9). Other rule-based algorithms, such as RP and RLF, returned a set of rules in which only the variables of Eq.2 were present.

Regarding computational time, it should be noted that the training phase took a few seconds for all the models, and interpretability took up to 3 hours.

### 3.3. Heart attack prediction

Finally, SIBILA is used to predict the probability of a patient suffering a heart attack. Data was imported from the Kaggle repository [34] and curated to model it as a binary classification problem.

After running all models, the highest scoring ones obtained similar accuracy: ANN (AUC=0.870), RF (AUC=0.895), RLF (AUC=0.810), RP (AUC=0.844) and XGBOOST (AUC=0.863). Contrary to them, DT (AUC=0.5), SVM (AUC=0.612) and KNN (AUC=0.723) achieved worse results and were disregarded. Then, two samples that RF predicted as class 0 or 1 with the highest probability (1.00) were analysed to identify the most critical features. RF was chosen as the reference model because it returned the highest AUC, and LIME was used due to its explanatory ability.

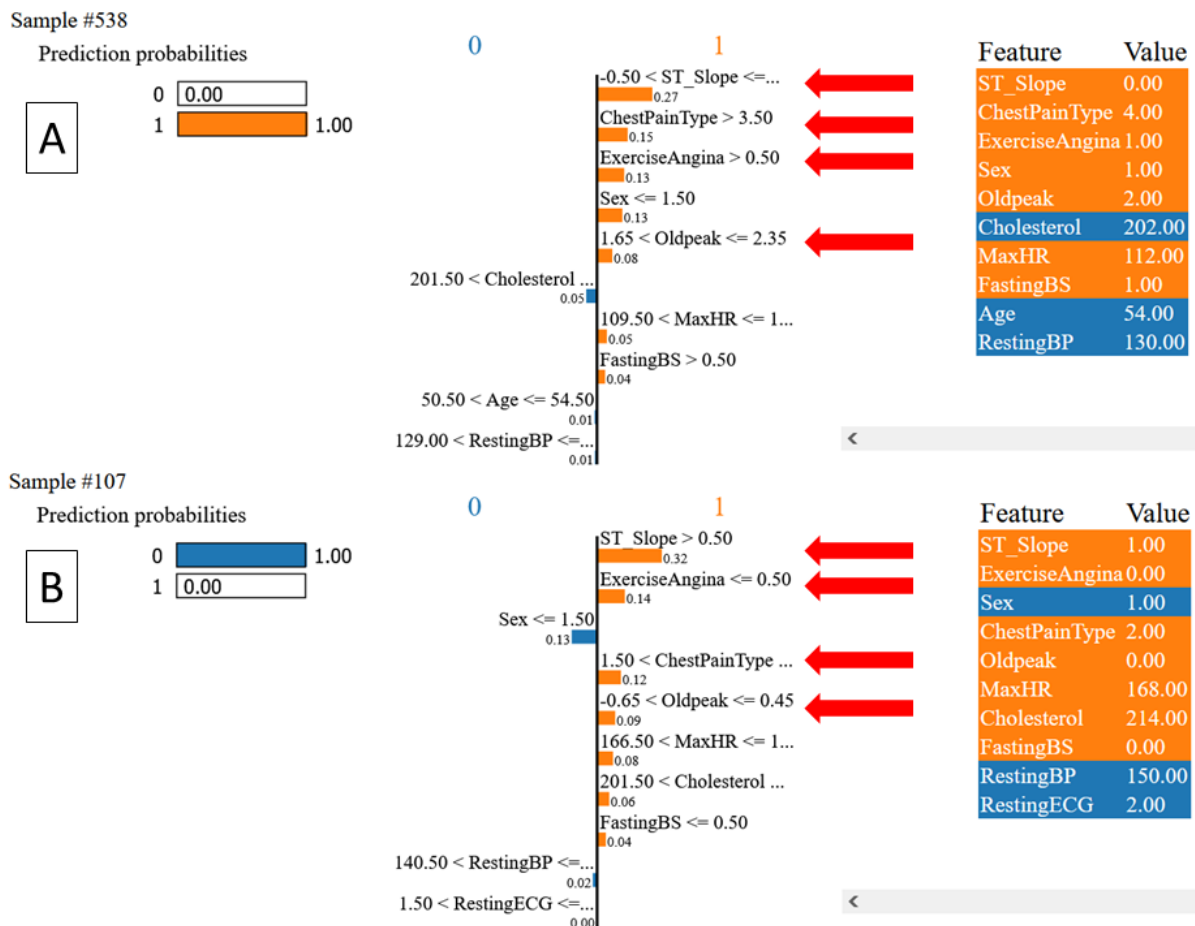


**Figure 10.** Features used by LIME to predict the probabilities of a heart attack. A) Sample classified as class 1; B) Sample classified as class 0. Red arrows point to the relevant features identified from the explanations.

LIME shows the actual values of each sample on the right. In the orange background are the features that lead to classifying the sample as class 1 (high probability of suffering an attack) and in the blue background are the ones classifying the sample as class 0 (low probability of suffering an attack). The left side shows the probability with which the model predicted that sample as class 0 or 1. The middle column depicts the explanation of the sample, including the rules and edge values extracted from the model. An orange bar means that, according to the actual value of the feature, the sample should be classified as class 1, and a blue bar represents the features that indicate that the sample should belong to class 0.

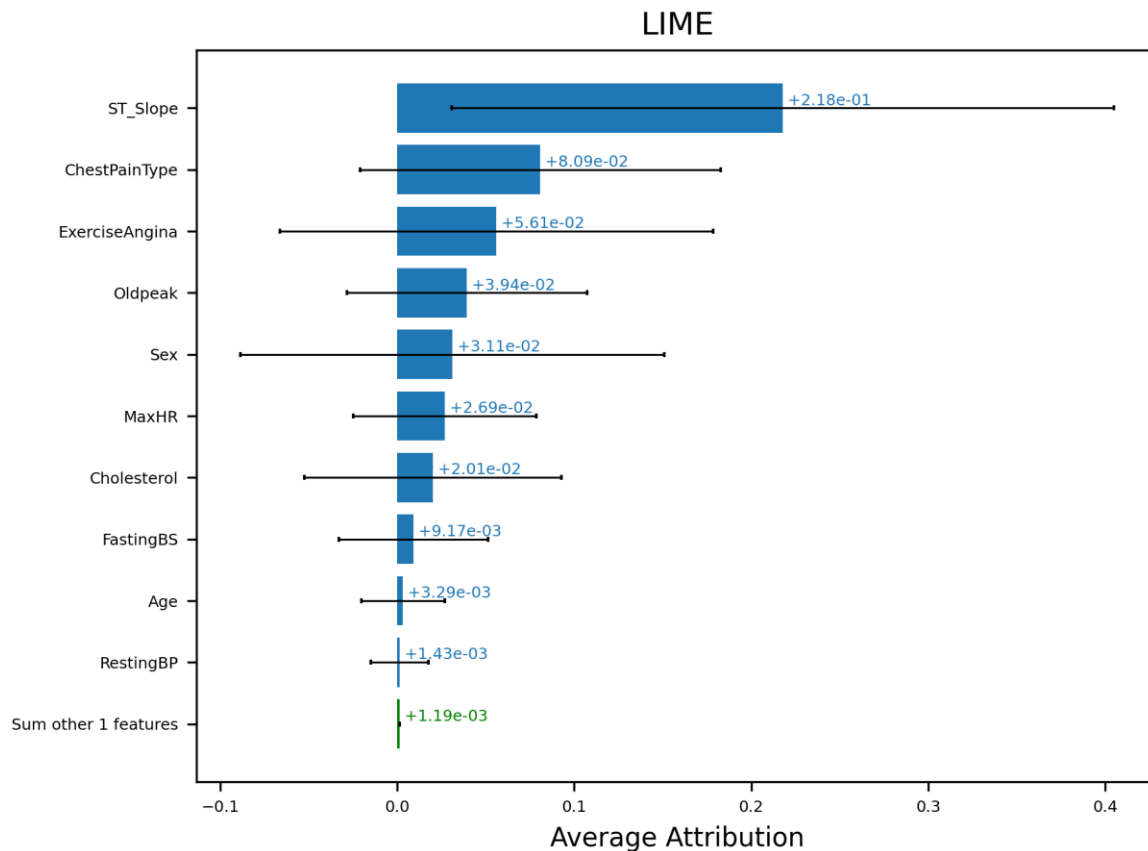
Based on this representation, Figure 10 shows two samples clearly classified as class 1 and 0, respectively. According to the actual values of Figure 10a, most of the features indicate that the sample represents a patient with a high probability of a heart attack (class 1), and as expected, the model classified the patient in that class. Next, looking at the most attributed features, it can be concluded that when ST\_Slope is around 0 (flat), ChestPainType is close to 4 (asymptomatic), ExerciseAngina is close to 1 (yes) and Oldpeak ranges between 1.65 and 2.35, the chances of suffering a heart attack are higher.

Figure 10b analyses the prediction of a patient with a low probability of suffering a heart attack. It is worth highlighting two findings:

- Only Sex, RestingBP and RestingECG indicate that the patient is not prone to suffering an attack.

- Although the features identified in Figure 10a remain in orange, they range differently. If ST\_Slope is close to 1 (upsloping), ExerciseAngina is far from 1 (no), ChestPainType ranges between 1.50 and 2.50 (atypical angina) and Oldpeak ranges between -0.65 and 0.45, the patient has few chances of suffering an attack.

Despite the overlapping in the features involved, it can be seen that both explanations are consistent and mutually exclusive. Therefore, we could conclude that ST\_Slope, ExerciseAngina, ChestPainType and Oldpeak are good markers to predict whether a patient will be at risk. Figure 11 summarises the average attributions given by LIME.



**Figure 11.** Top 10 features attributed by LIME. The X-axis shows the averaged attribution of each feature, and the Y-axis represents the top 10 most important features. Black horizontal lines depict the standard deviation of the attribution values given to the features.

In terms of performance, amongst the most accurate models, the most computationally expensive was ANN, which only took nearly 1 minute to train the model. Additionally, SIBILA took 39 extra minutes to compute interpretability with the slowest model (RP). Although SIBILA calculates interpretability for more samples in this dataset (1472 explanations) than in the previous one (400 explanations), it was three times faster. The reason could be that time spent on explaining the results is mainly linked to the number of input features rather than the number of samples because the algorithm must assess the importance of every individual feature. Based on this idea, the heart attack dataset, which only contains 11 features, should be much faster than the synthetic one, which stored 100 variables.

## 4. Discussion

The bike rental prediction example demonstrated that SIBILA can predict continuous outputs in regression problems. The results indicate that the total rentals depend on the number of reservations and the date. Since the dataset has not been curated, there is a high correlation between the date and other input features such as month, year, and season. In this example, the date seems to be the preferred feature to estimate the number of rentals. A cleaning stage could be performed on the dataset, and the results would be expected to remain similar.

To test the impact of noise in the predictions, a synthetic dataset was created for binary classification. The dataset consisted of 6 input features that determined the output class and 94 additional features to simulate noise in the data. Aiming to keep it as random as possible, it was populated with random numbers between 0 and 1 to avoid discrepancies in the range of the variables.

Despite the high number of disturbing features, SIBILA focused on the relevant features to identify the inherent rule (Eq. 1). Six models achieved the perfect classification (AUC=1), and four highlighted all the expected features within the ten most valued. The rest of highlighted variables could be a consequence of the random nature of the dataset. These results reveal that SIBILA is very little influenced by noise, which is essential when working with unexplored datasets whose internal rules are unknown.

Finally, a novel dataset with samples of patients who suffered or did not suffer a heart attack was used to simulate a real case. Five out of eight models outperformed the others with an AUC higher than 0.8. On the contrary, DT could only find a random classifier (AUC=0.5), probably because this model is too simplistic for a complex dataset. Among the most accurate models, RF performed the best (AUC=0.895). We therefore used it as a baseline to explore the results.

To prove the consistency of our explanations, LIME was chosen to interpret the results of the RF model. The idea behind LIME is to explain the behaviour of a model through the creation of explainable internal models [24]. A significant advantage of LIME is its ability to present edge values in the form of mathematical rules along with the actual values of each sample, which makes it easy to understand by non-experts. To explain the way the RF model worked, two samples, which were undoubtedly classified in both classes, have been selected.

**Table 4.** Rules found by LIME to predict the output class.

Sample #538 (Class 1)	#Sample 107 (Class 0)
$-0.50 < ST\_Slope \leq 0.50$	$ST\_Slope > 0.50$
$ChestPainType > 3.50$	$1.50 < ChestPainType \leq 2.50$
$ExerciseAngina > 0.50$	$ExerciseAngina \leq 0.50$
$Sex \leq 1.50$	$Sex \leq 1.50$
$1.65 < Oldpeak \leq 2.35$	$-0.65 < Oldpeak \leq 0.45$
$201.50 < Cholesterol \leq 278.50$	$201.50 < Cholesterol \leq 278.50$

109.50 < MaxHR <= 129.50	166.50 < MaxHR <= 183.00
FastingBS > 0.50	FastingBS <= 0.50
50.50 < Age <= 54.50	1.50 < RestingECG <= 2.50
129.00 < RestingBP <= 133.50	140.50 < RestingBP <= 182.50

LIME uses different rules to classify samples. However, most of them rely on the same variables (Table 4). As stated in Table 4, Sex and Cholesterol follow the same rule, so they are not good candidates to discriminate the class. In addition, Age and RestingECG are only applicable to samples of a given class. Thus, they may not be discriminatory enough. Consequently, there are only seven features which we should look at to make predictions like the model would do. Looking at the attribution given by LIME to these features (Fig. 10), ST\_Slope, ChestPainType, ExerciseAngina, and Oldpeak are the ones with the highest attribution. Therefore, interpretability suggests trusting them. Although they worked on different datasets, other manuscripts support these findings [35, 36].

## 5. Conclusions

ML and DL are powerful tools for decision-making systems, but their lack of interpretability remains a significant challenge. Without interpretability, physicians, lawyers, brokers, politicians, etc., will never trust ML/DL predictions, and society will miss the opportunity to take advantage of these techniques. Aiming to bring some light on this scenario, SIBILA has been developed. SIBILA consists of several ML/DL models and a web server accessible at no cost at <https://bio-hpc.ucam.edu/sibila/> to facilitate its use by any user. Its source code is available on Github (<https://github.com/bio-hpc/sibila>). In addition, to speed up its calculations, it can be run on supercomputing clusters with no extra configuration because all the necessary dependencies are packaged in a container.

The results prove that SIBILA performs well on both classification and regression problems. Furthermore, the results demonstrate that the interpretability calculation is a computationally expensive task that can take several hours, especially when the dataset has many input features. To cope with this inconvenience, that stage is parallelised on different nodes of an HPC cluster.

When suitably trained, SIBILA can be a good choice for doctors choosing the best practice for each patient. Its scope of application is not restricted, and it could be helpful in the treatment of diseases such as cardiovascular problems or cancer, as shown in section 3.3. Even more, it can be applied to biological or pharmaceutical datasets to find unknown biomarkers and effective drug combinations.

## Source code

The source code is available at <https://github.com/bio-hpc/sibila.git>.

## Funding

This work has been funded by grants from the European Project Horizon 2020 SC1-BHC-02-2019 [REVERT, ID:848098]; Fundación Séneca del Centro de Coordinación de la Investigación de la Región de Murcia [Project 20988/PI/18]; and Spanish Ministry of Economy and Competitiveness [CTQ2017-87974-R].

## Declaration of competing interest

The authors declare no competing interest.

## Acknowledgements

This work has been funded by grants from the European Project Horizon 2020 SC1-BHC-02-2019 [REVERT, ID:848098]; Fundación Séneca del Centro de Coordinación de la Investigación de la Región de Murcia [Project 20988/PI/18]; and Spanish Ministry of Economy and Competitiveness [CTQ2017-87974-R]. Supercomputing resources in this work were supported by the Poznan Supercomputing Center's infrastructures, the e-infrastructure program of the Research Council of Norway, and the supercomputing centre of UiT—the Arctic University of Norway, by the Plataforma Andaluza de Bioinformática of the University of Málaga, the supercomputing infrastructure of the NLHPC (ECM-02, Powered@NLHPC), and the Extremadura Research Centre for Advanced Technologies (CETA-CIEMAT), funded by the European Regional Development Fund (ERDF). CETA-CIEMAT is part of CIEMAT and the Government of Spain.

## References

- [1] Y. Xin, L. Kong, Z. Liu, Y. Chen, Y. Li, H. Zhu, M. Gao, H. Hou, C. Wang. Machine Learning and Deep Learning. *IEEE Access*, 6 (2018), pp. 35365-35381, 10.1109/ACCESS.2018.2836950
- [2] T. Ching, D. S. Himmelstein, B. K. Beaulieu-Jones, A. A. Kalinin, B. T. Do, G. P. Way, E. Ferrero, P.-M. Agapow, M. Zietz et al. Opportunities and obstacles for deep learning in biology and medicine. *J. R. Soc. Interface*, 15(141) (2018), pp. 20170387, 10.1098/rsif.2017.0387
- [3] Q. Bai, J. Ma, S. Liu, T. Xu, A.J. Banegas-Luna, H. Pérez-Sánchez, Y. Tian, J. Huang, H. Liu, X. Yao. WADDAICA: A webserver for aiding protein drug design by artificial intelligence and classical algorithm. *Comput. Struct. Biotechnol. J.*, 19 (2021), pp. 10.1016/j.csbj.2021.06.017
- [4] A.C. Mater, M.L. Coote. Deep Learning in Chemistry. *J. Chem. Inf. Model.*, 59(6) (2019), pp. 2545-2559, 10.1021/acs.jcim.9b00266
- [5] G.B. Goh, N.O. Hodas, A. Vishu. Deep learning for computational chemistry. *J. Comput. Chem.*, 38(16) (2017), pp. 1291-1307, 10.1002/jcc.24764
- [6] R. Miotto, F. Wang, S. Wang, X. Jiang, J.T. Dudley. Deep learning for healthcare: review, opportunities and challenges. *Brief. Bioinform.*, 19(6) (2018), pp. 1236-1246, 10.1093/bib/bbx044
- [7] J. Zou, M. Huss, A. Abid, P. Mohammadi, A. Torkamani, A. Telenti. A primer on deep learning in genomics. *Nat. Genet.*, 51(1) (2019), pp. 12-18, 10.1038/s41588-018-0295-5

- [8] G. Eraslan, Z. Avsec, J. Gagneur, F.J. Theis. Deep learning: new computational modelling techniques for genomics. *Nat. Rev. Genet.*, 20(7) (2019), pp. 389-403, 10.1038/s41576-019-0122-6
- [9] S. Min, B. Lee, S. Yoon. Deep learning in bioinformatics. *Brief. Bioinform.*, 18(5) (2017), pp. 851-869, 10.1093/bib/bbw068
- [10] E. Gawehn, J.A. Hiss, G. Schneider. Deep Learning in Drug Discovery. *Mol. Inform.*, 35(1) (2016), pp. 3-14, 10.1002/minf.201501008
- [11] E.H.B. Maia, L.C. Assis, T.A. de Oliveira, A.M. da Silva, A.G. Taranto. Structure-Based Virtual Screening: From Classical to Artificial Intelligence. *Front. Chem.*, 8 (2020), pp. 343, 10.3389/fchem.2020.00343
- [12] L. Patel, T. Shukla, X. Huang, D.W. Ussery, S. Wang. Machine Learning Methods in Drug Discovery. *Molecules*, 25(22) (2020), pp. 5277, 10.3390/molecules25225277
- [13] C. Pérez-Gandía, G. García-Sáez, D. Subías, A. Rodríguez-Herrero, E.J. Gómez, M. Rigla, M.E. Hernando. Decision Support in Diabetes Care: The Challenge of Supporting Patients in Their Daily Living Using a Mobile Glucose Predictor. *J. Diabetes Sci. Technol.*, 12(2) (2018), pp. 243-250, 10.1177/1932296818761457
- [14] Y. Lee, R.M. Raggett, R.B. Mansur, J.J. Boutilier, J.D. Rosenblat, A. Trevizol, E. Brietzke, K. Lin, Z. Pan, M. Subramaniapillai, T.C.Y. Chan, D. Fus, C. Park, N. Musial, H. Zuckerman, V.C.H. Chen, R. Ho, C. Rong, R.S. McIntyre. Applications of machine learning algorithms to predict therapeutic outcomes in depression: A meta-analysis and systematic review. *J. Affect. Disord.*, 241 (2018), pp. 519-532, 10.1016/j.jad.2018.08.073
- [15] M. Misawa, S.E. Kudo, Y. Mori, T. Cho, S. Kataoka, A. Yamauchi, Y. Ogawa, Y. Maeda, K. Takeda, K. Ichimasa, H. Nakamura, Y. Yagawa, et al. Artificial Intelligence-Assisted Polyp Detection for Colonoscopy: Initial Experience. *Gastroenterology*, 154(8) (2018), pp. 2027-2029, 10.1053/j.gastro.2018.04.003
- [16] K. Ichimasa, S.E. Kudo, Y. Mori, M. Misawa, S. Matsudaira, Y. Kouyama, T. Baba, E. Hidaka, K. Nakamura, T. Hayashi, T. Kudo, T. Ishigaki, Y. Yagawa, et al. Artificial intelligence may help in predicting the need for additional surgery after endoscopic resection of T1 colorectal cancer. *Endoscopy*, 50(3) (2018), pp. 230-240, 10.1055/s-0043-122385
- [17] P. Hamet, J. Tremblay. Artificial intelligence in medicine. *Metabolism*, 69S (2017), pp. S36-S40, 10.1016/j.metabol.2017.01.011
- [18] N.J. Schork. Artificial Intelligence and Personalized Medicine. *Cancer Treat. Res.*, 178 (2019), 265-283, 10.1007/978-3-030-16391-4\_11
- [19] O. Khan, J.H. Badhiwala, G. Grasso, M.G. Fehlings. Use of Machine Learning and Artificial Intelligence to Drive Personalized Medicine Approaches for Spine Care. *World Neurosurg.*, 140 (2020), pp. 512-518, 10.1016/j.wneu.2020.04.022
- [20] G.S. Handelman, H.K. Kok, R.V. Chandra, A.H. Razavi, M.J. Lee, H. Asadi. eDoctor: machine learning and the future of medicine. *J. Intern. Med.*, 284(6) (2018), pp. 603-619, 10.1111/joim.12822
- [21] C. Zippel, S. Bohnet-Joschko. Rise of Clinical Studies in the field of Machine Learning: A Review of Data Registered in ClinicalTrials.gov. *Int. J. Environ. Res. Public Health*, 18 (2021), pp. 5072, 10.3390/ijerph18105072
- [22] R. Miotto, F. Wang, S. Wang, X. Jiang, J.T. Dudley. Deep learning for healthcare: review, opportunities and challenges. *Brief. Bioinform.*, 19(6) (2018), pp. 1236-1246, 10.1093/bib/bbx044
- [23] Permutation\_importance. [https://scikit-learn.org/stable/modules/generated/sklearn.inspection.permutation\\_importance.html?highlight](https://scikit-learn.org/stable/modules/generated/sklearn.inspection.permutation_importance.html?highlight)

[ht=permutation\\_importance#sklearn.inspection.permutation\\_importance](#). Accessed on 25<sup>th</sup> February 2022.

[24] C. Molnar. Interpretable Machine Learning. A Guide for Making Black Box Models Explainable. 2nd Edition.

[25] Lime. <https://github.com/marcotcr/lime>. Accessed on 25<sup>th</sup> February 2022.

[26] SHAP. <https://shap.readthedocs.io/en/latest/index.html>. Accessed on 25<sup>th</sup> February 2022.

[27] Alibi - Integrated Gradients.

<https://docs.seldon.io/projects/alibi/en/latest/methods/IntegratedGradients.html>. Accessed on 10<sup>th</sup> February 2022.

[28] Diverse Counterfactual Explanations (DiCE) for ML. <http://interpret.ml/DiCE/>. Accessed on 25<sup>th</sup> February 2022.

[29] Plot\_partial\_dependence. [https://scikit-learn.org/stable/modules/generated/sklearn.inspection.plot\\_partial\\_dependence.html?highlight=partial%20dependence%20plot#sklearn.inspection.plot\\_partial\\_dependence](https://scikit-learn.org/stable/modules/generated/sklearn.inspection.plot_partial_dependence.html?highlight=partial%20dependence%20plot#sklearn.inspection.plot_partial_dependence). Accessed on 25<sup>th</sup> February 2022.

[30] Accumulated Local Effects.

<https://docs.seldon.io/projects/alibi/en/stable/methods/ALE.html>. Accessed on 25<sup>th</sup> February 2022.

[31] Singularity container. <https://sylabs.io/guides/3.5/user-guide/index.html>. Accessed on 25<sup>th</sup> February 2022.

[32] G. Hu, Y. Zhang, W. Chen. Exploring the Performance of Singularity for High-Performance Computing Scenarios. 2019 IEEE 21st International Conference on High-Performance Computing and Communications; IEEE 17th International Conference on Smart City; IEEE 5th International Conference on Data Science and Systems (HPCC/SmartCity/DSS), (2019), pp. 2587-2593, 10.1109/HPCC/SmartCity/DSS.2019.00362

[33] Y. Liu, S. Khandagale, C. White, W. Neiswanger. Synthetic Benchmarks for Scientific Research in Explainable Machine Learning. arXiv:2106.12543v4, doi.org/10.48550/arXiv.2106.12543

[34] fedesoriano. (September 2021). Heart Failure Prediction Dataset. Retrieved 10<sup>th</sup> February 2022 from <https://www.kaggle.com/fedesoriano/heart-failure-prediction>.

[35] S.B. Patil, Y.S. Kumaraswamy. Extraction of Significant Patterns from Heart Disease Warehouses for Heart Attack Prediction. International Journal of Computer Science and Network Security, 9(2) (2009), pp. 228-235.

[36] H.D. Masethe, M.A. Masethe. Prediction of Heart Disease using Classification Algorithms. Lect. Notes Eng. Comp., 2, 2014, pp.809-812.